Influence of pressure and velocity perturbations on the heat release fluctuations for coaxial GH_2/GO_2 injection

M. Schmid⋆ *and T. Sattelmayer*⋆
⋆*Lehrstuhl für Thermodynamik, Technische Universität München*
Boltzmannstraße 15, D-85748 Garching

Abstract

Determination of the flame response to acoustic fluctuations is a crucial task during the stability analysis of rocket engines. A method to compute the flame response of single injectors to tangential pressure and velocity fluctuations has been developed. It can be used to study the influence of these fluctuations on the heat release rate. Furthermore, free parameters of flame response models, such as those of Crocco's n-τ-model [2], can be determined and used in acoustic simulations of complete rocket combustion chambers. Excitation methods for pressure and velocity fluctuations are presented. As an example, the response of the heat release rate of a gaseous hydrogen/oxygen flame to acoustic perturbations is shown. The fluctuations are excited via periodically fluctuating source terms in the momentum and/or continuity equations.

1. Nomenclature

Latin symbols

A	$[m^2]$	Area
c	$[m/s]$	Speed of sound
$\dot{e}$	$[W/m^2]$	Energy source term
f	$[1/s]$	Frequency
F	$[N]$	Force
k	$[1/m]$	Wave number
J_1	$[-]$	Bessel function of first kind and first order
$\dot{m}$	$[kg/s]$	Mass flow rate
n	$[-]$	Proportionality factor
$\vec{n}_y$	$[-]$	Normal vector in y-direction
p	$[bar]$	Pressure
$\dot{s}_v$	$[N/m^3]$	Momentum source term for velocity excitation
$\dot{s}_p$	$[N/m^2]$	Momentum source term for pressure excitation
s_{11}	$[-]$	First root of $\partial J_1(r)/\partial r$; $s_{11} = 1.8412$
t	$[s]$	Time
v	$[m/s]$	Velocity
V	$[m^3]$	Volume
x	$[m]$	Axial coordinate
y	$[m]$	Transversal coordinate

Greek symbols

ϕ	$[rad]$	Phase
ρ	$[kg/m^3]$	Density
ω	$[1/s]$	Angular frequency ($\omega = 2\pi f$)

Indices

p	Pressure
v	Velocity

Superscripts

$\cdot'$	Fluctuating quantity
$\bar{\cdot}$	Mean value
$\hat{\cdot}$	Amplitude
$\tilde{\cdot}$	Dimensionless value

Abbreviations

APE	Acoustic Perturbation Equations
CAA	Computational Aero Acoustics
CFD	Computational Fluid Dynamics
EDC	Eddy Dissipation Concept
FFT	Fast Fourier Transform
LEE	Linearized Euler Equations
$RANS$	Reynolds Averaged Navier-Stokes
RMS	Root Mean Square

2. Introduction

A key issue during the development process of rocket engines is the verification of combustion stability. Combustion instabilities appear if acoustic fluctuations in the combustion chamber interact with the combustion process and yield a fluctuating heat release rate. If these fluctuations are in phase with the pressure fluctuations, the acoustic fluctuations can rise up to levels, which are able to destroy the whole combustion chamber. Based on the experience regarding combustion instability modeling in the field of stationary gas turbines as well as rocket engines, the *Lehrstuhl für Thermodynamik* of the *Technische Universität München* has selected a coupled CAA/CFD-approach for the analysis of combustion stability. This hybrid approach is chosen, because simulations of complete rocket combustion chambers with up to several hundreds of injectors resolved in detail will remain numerically too costly for an industrial application even in the near future.
The wave propagation in the combustion chamber is calculated by an CAA-code whereas the flame coupling is determined via CFD-simulations. A numerical tool, PIANO-SAT, has been developed with the aim of getting a better understanding of the physical processes yielding to these instabilities and to be finally able to predict numerically the level of instability in rocket engines. This three-dimensional code, which operates in the time domain, is based on the PIANO[i]-code [3] and solves either the **A**coustic **P**erturbation **E**quations (**APEs**) or the **L**inearized **E**uler **E**quations (**LEE**). The general feasibility of simulating stability limits in rocket engines with PIANO-SAT has been shown for the first time by Pieringer [10]. One major problem in the simulation is the modeling of the feedback loop which couples the acoustic pressure and velocity fluctuations to the heat release rate. Three-dimensional, unsteady simulations using the **R**eynolds **A**veraged **N**avier-**S**tokes equations (**RANS**) are used to investigate this coupling. The general feasibility of calculating flame transfer functions via numerical simulations has previously been demonstrated for gas turbine burners by Tay [14]. To study the coupling of acoustics and heat release, it is necessary to know the acoustic field in the combustion chamber, especially close to the faceplate. The eigenfrequencies and mode shapes of a combustion chamber can be determined with acoustic simulations using PIANO-SAT or with simple analytical solutions of the wave equation including mean flow. Then, these known frequencies and mode shapes can be used in single injector simulations to study the flame response.
Recently, excitation methods have been developed to impose this known acoustic field on computational domains of single injectors with periodic boundaries. These methods use source terms in the momentum and/or continuity equations. After the description of the numerical implementation of forcing, results of the influence of pressure and velocity fluctuations on the heat release rate are shown.

3. Excitation methods

As already mentioned, the aim of the presented study is to develop excitation methods for transverse modes in single injector configurations with periodic conditions at the boundaries parallel to the main flow. Previous publications on excitation methods were focused on purely longitudinal modes ([8] and [4]) or did not include periodic boundaries ([5] and [15]). In the following, excitation methods for pressure and velocity fluctuations are presented. Typically, the geometrical length scales in the transverse direction of rocket injectors are much smaller than the acoustic wave length in this direction. It is assumed that the fluctuations have a constant amplitude and no phase shift in axial direction. This assumption holds only in the case of a vanishing Mach-number and at a frequency equal to the cut-on-frequency of transverse modes in the corresponding combustion chamber. However, an extension of the methods to simulations including gradients and phase shifts in axial direction seems to be easily possible. Then, the methods will be applicable to any mean Mach number. For the velocity fluctuations, gradients in the transverse direction are neglected, too.

3.1 Pressure excitation

Acoustic pressure and velocity fluctuations are connected via mass and momentum conservation. Local pressure differences lead to an acceleration of the fluid. Figure 1 shows the spatial distributions of acoustic fluctuations. The injector width is indicated by the two dotted gray vertical lines. As already mentioned, the injector dimensions are in general much smaller than the acoustic wave length. The shown dimension in the transverse direction y in Fig. 1 is chosen equal to $1/20$ of the wave length. Pressure fluctuations are spatially symmetrical around the pressure anti-node for a standing wave (cosine-shape, solid line). In contrast, velocity fluctuations are spatially anti-symmetrical around the pressure anti-node (sine-shape, dashed line). This means, that the velocity fluctuations have opposite signs on opposite

[i]Provided by the DLR Braunschweig, Institute of Aerodynamics and Flow Technology, Prof. Dr.-Ing. Jan Delfs

sides of the pressure anti-node ($y = 0$) during the whole acoustic oscillation period.

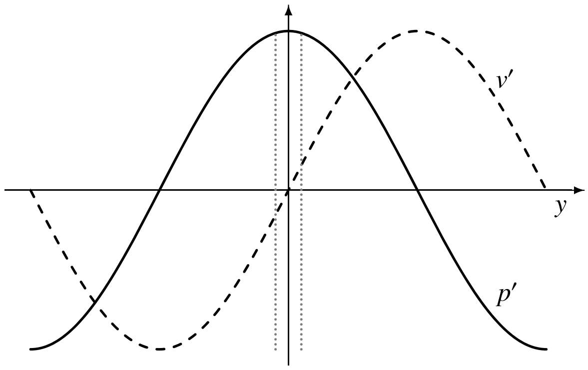

Figure 1: Sketch of the pressure anti-node

The modeling approach for the pressure excitation method is given in the following.
As already explained, the aim is to impose pressure fluctuations of the following form (Eq. 1)

$$p' = \hat{p} \sin(\omega t) \cos(ky) \tag{1}$$

with a pressure anti-node at the axis of the injector ($y = 0$) and with the wave number defined as $k = \frac{\omega}{c}$. These pressure fluctuations in the domain result from velocity fluctuations at the boundaries in the transverse direction. The velocity fluctuations add mass to the simulation domain at both sides in one half of the oscillation period. In the other half of the period, they extract mass. Therefore, these velocity fluctuations can be interpreted as a mass source or sink term. In addition, the mass source terms lead to corresponding momentum and energy source terms, too. The basic idea of the pressure excitation method (velocity fluctuations and source terms at the boundaries) is shown in Fig. 2.

Figure 2: Sketch of the pressure excitation method

The excitation method presented above can mathematically be described starting from the linearized momentum equation in the transverse direction, perpendicular to the main flow (Eq. 2). Mean flow in the transverse direction is neglected. Additionally, gradients of the mean values are neglected for the derivation of the excitation method.

$$\frac{\partial v'}{\partial t} = -\frac{1}{\overline{\rho}} \frac{\partial p'}{\partial y} \tag{2}$$

Introducing Eq. 1 into Eq. 2 yields velocity fluctuations of the following form (Eq. 3).

$$v' = \frac{\hat{p}}{\overline{\rho} c} \cos(\omega t) \sin(-ky) \tag{3}$$

This finally yields an area-weighted mass source term $\left[kg/m^2\right]$ at the periodic boundaries (Eq. 4).

$$\frac{\dot{m}'}{A} = v'\overline{\rho} = \frac{\hat{p}}{c} \sin(\omega t) \,|\sin(-ky)\ \vec{n}_y\,| \tag{4}$$

The normal vector in the mass source term appears as the boundary is not necessarily perpendicular to the fluctuating velocity. The used wave number is not equal to the local wave length in the real chamber. Instead, it depends on the local position of the injector in radial and circumferential direction as well as the Mach number in the chamber. A more detailed modeling of the wave length for the excitation method has no influence as long as the wave length is much

shorter than the injector dimensions in transverse direction.
The mass source term has been implemented with the corresponding momentum and energy source terms. The momentum source terms are calculated with a mean velocity in the axial direction equal to the velocity at the outlet and with the local velocity fluctuation in the transverse direction. For the energy source term, an isentropic fluctuating temperature is assumed. The injection direction at the face plate fluctuates with the local acoustic velocity fluctuations.
As the pressure amplitude and frequency are known a priori, a periodically fluctuating pressure at the outlet is set.
Using these boundary conditions in the CFD-code leads to velocity fluctuations in anti-phase at opposite boundaries of the domain. Finally, this results in the desired pressure fluctuations according to Eq. 1.

3.2 Velocity excitation

To force velocity fluctuations, a harmonically fluctuating momentum source term in the momentum balance equation in the transverse direction is used in the domain. As periodic boundaries are applied, velocity fluctuations in the domain yield no pressure fluctuations at the boundaries. The fluid leaves the domain and enters at the opposite side. To excite velocity fluctuations in the form of Eq. 5,

$$v' = \hat{v} \sin(\omega t) \tag{5}$$

the following formulation of the source term is used (Eq. 6):

$$\dot{s}_v = \overline{\rho}\hat{v}\omega \cos(\omega t) \tag{6}$$

The source term can be interpreted as follows: A momentum source term corresponds to a force per volume. As the consequence, it can be written as the product of density and acceleration. Acceleration is finally the time derivative of the velocity fluctuation (Eq. 7).

$$\dot{s}_v = \frac{F}{V} = \overline{\rho}\frac{\partial v'}{\partial t} \tag{7}$$

The density can be taken as the local density or a global reference density. The first case leads to a constant amplitude of the velocity fluctuations in the whole domain and corresponds to a constant acceleration in the domain. The second case generates a constant amplitude of the momentum source term in the domain and yields a constant force per volume. The second is better suited for simulations of rocket combustion. The chamber acoustics impose a constant momentum source term in the domain. As a consequence, different velocity fluctuation amplitudes appear in regions with different densities.
After the implementation into *ANSYS CFX*, several test cases have been simulated. A hexagonal simulation domain, similar to the test case presented later (Fig. 3), has been used. A constant mean flow over the cross section has been imposed. The results showed that the excitation yields the prescribed pressure and velocity fluctuations for different mean Mach numbers as well as excitation frequencies and amplitudes. Furthermore, the pressure fluctuations yield isentropic fluctuations of temperature and densities, which are characteristic for acoustic fluctuations.

4. Testcase

A typical coaxial injector has been chosen to test the excitation methods and to perform some preliminary investigations on the influence of acoustic fluctuations on the heat release rate. In the following, the geometry and mesh of the test case as well as the used models for turbulence and combustion are presented. Finally, the flow conditions are given, too.

4.1 Geometry and mesh

As already explained before, hexagonal domains of single injectors with periodic boundaries are used to approximate the global structure of the faceplate. The length of the domain is 200 *mm*. The grid consists of about 223000 cells. Figure 3 shows the mesh. The blue part is the oxidizer inlet, the red one the fuel inlet. The green and yellow portion of the faceplate are walls. Massflow inlets and an opening outlet with fixed static pressure are used.

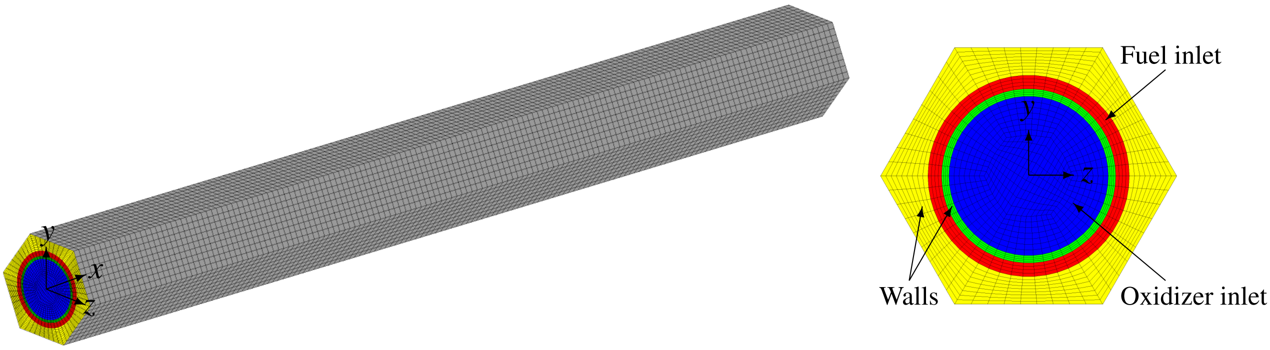

Figure 3: Mesh of the test case

4.2 Details of the simulations

Simulations were made with *ANSYS CFX* using the RANS-equations together with the k-ϵ turbulence model and a single reaction EDC reaction scheme (Eq. 8), which was developed by Astrium [7].

$$H_2 + xO_2 \rightarrow aH_2O + bH + cOH \tag{8}$$

The coefficients of this reaction equation are adapted to best fit the final combustion temperature for a mixture ratio of $O/F = 6$. The ideal gas law was used for all species.
The High Resolution Advection Scheme and a Second Order Backward Euler Transient Scheme as well as First Order Turbulent Numerics are used. The time step is in general defined such that 100 points per period of the excitation frequency are calculated. For higher excitation amplitudes, the time step is reduced to achieve RMS-values of the convergence criteria below 10^{-5}.

4.3 Flow conditions

The flow conditions are chosen similar to the RCM-2-Testcase ([13]). The mixture ratio is changed to $O/F = 6$, because the available reaction scheme was adapted for that ratio. A density ratio of $\rho_{Ox}/\rho_{Fu} = 24$ and a momentum ratio $J = \left(\rho_{Ox} v_{Ox}^2\right) / \left(\rho_{Fu} v_{Fu}^2\right) = 0.25$ are used. Table 1 gives an overview of the injection conditions as well as the geometrical dimensions. For hydrogen, the inner and outer diameter of the injection annulus are given. A mean pressure of 10 *bar* is imposed at the outlet boundary.

Table 1: Injection parameters

	Massflow $[g/s]$	**Velocity** $[m/s]$	**Temperature** $[K]$	**Diameter** $[mm]$
Oxygen	26.29	14	200	10.76
Hydrogen	4.38	137	300	11.76/13.60

The inner part of the injector upstream of the faceplate is currently not taken into account. The influence of this upstream part on the flame response will be part of future studies.

5. Results

A total of 15 simulations have been carried out with both excitation methods and with different excitation amplitudes and frequencies. The aim was to test the excitation methods together with combustion, i.e. varying temperature and chemical composition. A second aim was to perform some preliminary studies on the influence of acoustic fluctuations on the heat release rate.
The mean flow field is shown first in the next section. Later, the used flame model for the dynamic flame behavior is presented. Finally, the different test cases and a comparison of the results are given.

5.1 Mean flow field

Figures 4 and 5 show contour plots of the distribution of temperature as well as molar reaction rate. It can be recognized that both are not affected by the hexagonal structure of the domain, i.e. the flow field is rotationally symmetric, as it can be expected. The overall flame structure is visible in Fig. 4. It can be seen in Fig. 5 that the reaction process is

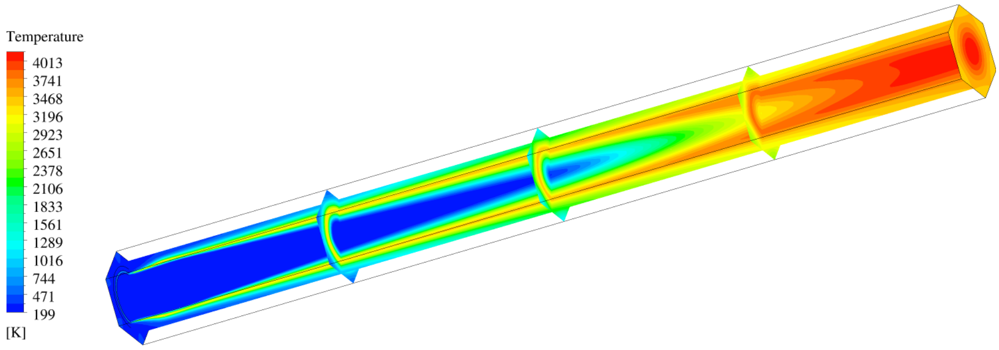

Figure 4: Temperature

nearly completed at the end of the simulation domain. The highest reaction rates are observed near the injection plane.

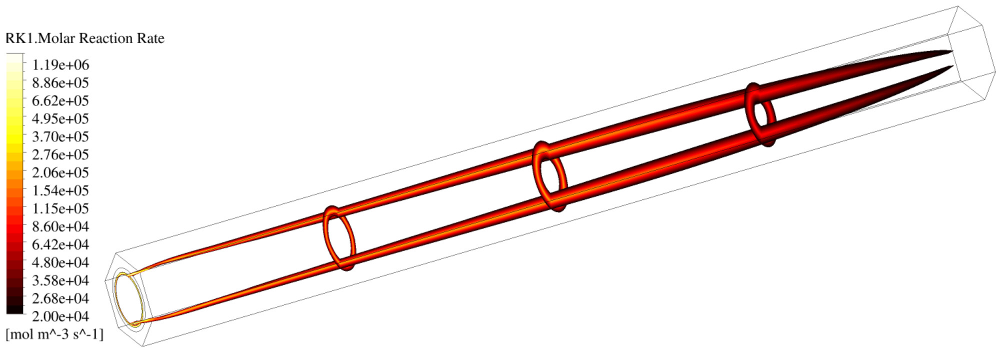

Figure 5: Reaction rate

5.2 Flame model

Crocco's time-lag-model [2] is used to model the dynamic flame behavior as a function of the acoustic excitation. It is extended to take the influence of pressure as well as velocity fluctuations into account. The first part couples the heat release fluctuations to pressure fluctuations (Eq. 9), the second (Eq. 10) gives a relation between transverse velocity fluctuations and heat release fluctuations. In a linear case, both can be superimposed and give finally the total heat release rate fluctuations (Eq. 11). The free parameters (n and τ) are calculated using the previously presented excitation methods. The model can be used in acoustic simulations of complete combustion chambers. Furthermore, it allows simple comparisons between simulations with different frequencies and amplitudes.

$$\tilde{\dot{q}}'_p(t) = n_p^{11}\tilde{p}'\left(t-\tau_p^{11}\right) \tag{9}$$

$$\tilde{\dot{q}}'_v(t) = n_v^{11}\tilde{v}'\left(t-\tau_v^{11}\right) \tag{10}$$

$$\tilde{\dot{q}}'(t) = \tilde{\dot{q}}'_p(t) + \tilde{\dot{q}}'_v(t) \tag{11}$$

Here, the dimensionless heat release rate is defined as $\tilde{\dot{q}}' = Q/\bar{Q} - 1$ and the nondimensional pressure fluctuations are equal to $\tilde{p}' = p/\bar{p} - 1$.

The nondimensionalization of the pressure fluctuations with the mean pressure is quite intuitive, but it is not for the velocity fluctuations. The sonic velocity could be used. However, the resulting dimensionless amplitudes of pressure and velocity fluctuation are not comparable. Therefore, another way has been chosen. The velocity amplitude is transformed in dimensionless form via Eq. 12.

$$\tilde{v}'(t) = \frac{v(t)\bar{\rho}c}{\bar{p}s_{11}} - 1 \tag{12}$$

The mean values for pressure, sonic velocity and density are taken from the outlet of the domain. This nondimensional form has been chosen to make the dimensionless amplitudes of pressure and velocity excitation comparable. The relation can be derived using the analytical solution for a cylinder [9] without mean flow and at a frequency equal to the cut-on-frequency of the first transverse mode. Figure 6 shows the location of the two considered injectors. The figure is colored with the pressure mode shape. Both injectors are situated near the outer wall, one is exposed to pure pressure fluctuations, the other one purely to velocity fluctuations. Pressure fluctuation levels are usually known as they can be determined experimentally quite easily. If the two dimensionless amplitudes are equal in simulations using the previously presented excitation methods, the dimensional pressure and velocity amplitudes correspond to the amplitudes in the same chamber at a given pressure fluctuations level but at different circumferential positions in the chamber.
As shown later, the flame model parameters n and τ depend on the frequency. The time signal of the pressure fluctuations in a combustion chamber consists always of the superposition of several different frequencies. Therefore, results of acoustic simulations with the above presented feedback model have to be interpreted very carefully. Further developments are necessary to model the complex flame behavior in the time domain.
Results of the two excitation methods presented previously (pressure and velocity fluctuations) are discussed in the following.

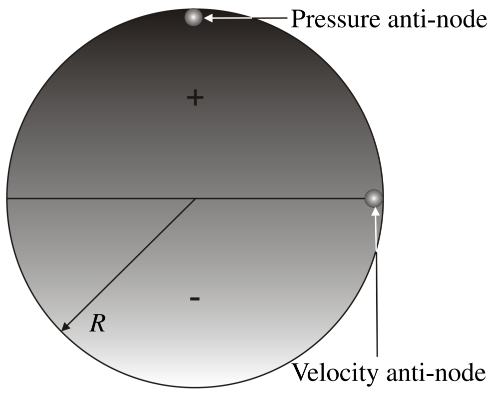

Figure 6: Sketch of faceplate

5.3 Overview of the test cases

This section gives an overview of the different simulations. The results are discussed in detail in the following sections. All simulated test cases are shown in Tab. 2. The first column indicates the index of the specific simulations. Columns 3-4 show the parameters of the excitation methods. The results are given in columns 5-10 in terms of flame model parameters n and τ as well as the phase between heat release and acoustic fluctuations divided by 2π ($\phi/(2\pi) = f\tau$). The proportionality factor n and the time lag τ are determined from Fast-Fourier-Transforms of the volume-integrated heat release rate and the pressure or velocity signal at the outlet. Index 11 means, that amplitude and phase of excitation and response are extracted at the same frequency. For the values with index 21, amplitude and phase of the heat release of twice the excitation frequency are correlated with the values from the excitation signal at the excitation frequency. Simulations 1-6 are forced with the previously presented pressure excitation method. Cases 7 and 8 are excited only at the outlet. No source terms at the boundaries are imposed. Instead, a harmonically fluctuating pressure is set at the outlet. This is referred to as longitudinal forcing in the following. The previously presented excitation method with source terms is used once again in test case 9. Here, the pressure amplitude is linearly increased by 0.2% per period. Test cases 10 to 15 are all excited with the velocity excitation method.
The response of the simulations shows the expected behavior in terms of frequency, amplitude and phase along the axis

as well as in transverse direction. It can be stated that the excitation methods work well in the case of an homogeneous flow as well as in the case with combustion and a very inhomogeneous flow field.

Table 2: Test case overview and results

No.	Exc.[ii]	f [Hz]	Ampl. [%]	$\mathbf{n^{11}_{p/v}}$	$\tau^{11}_{p/v}$	$\phi^{11}_{p/v}/(2\pi)$	$\mathbf{n^{21}_{p/v}}$	$\tau^{21}_{p/v}$	$\phi^{21}_{p/v}/(2\pi)$	Remark
1	P	2000	0.1	1.8	0.4	0.9	-	-	-	
2	P	3000	0.1	0.7	0.3	0.9	0.5	0.05	0.15	
3	P	4000	0.1	1.0	0.2	0.9	0.2	0.04	0.16	
4	P	5000	0.1	1.4	0.2	0.9	-	-	-	
5	P	4000	1.0	0.7	0.2	0.9	0.14	0.04	0.16	
6	P	4000	5.0	1.1	0.2	0.9	-	-	-	
7	P	4000	0.1	4.8	0.2	0.9	-	-	-	Longitudinal
8	P	4000	1.0	4.8	0.2	0.9	-	-	-	Longitudinal
9	P	4000	6.3	1.0	0.2	0.9	-	-	-	Transient Amplitude
10	V	2000	0.02	-	-	-	1.22	0.10	0.19	
11	V	3000	0.02	-	-	-	0.57	0.08	0.24	
12	V	4000	0.02	-	-	-	0.15	0.05	0.20	
13	V	5000	0.02	-	-	-	0.09	0.03	0.13	very weak response
14	V	3000	0.19	-	-	-	0.24	0.06	0.18	
15	V	4000	0.19	-	-	-	0.31	0.05	0.20	

5.4 Pressure Fluctuations

In addition to the mass source term, values for the corresponding energy and momentum of this mass source have to be calculated. For this purpose, temperature, turbulence properties and mass fractions have to be fixed for the source terms. Currently, global mean values of the outlet are used. However, it is planned to use the local values at the boundary in the future, which would be more physical.

5.4.1 Frequency dependence at 0.1% amplitude

Test cases 1-4 show the influence of the forcing frequency on flame response. The results show a constant phase, but different time lags for different excitation frequencies. The amplitude of the response depends also on the frequency (see Tab. 2). It shows a minimum between 3000 Hz and 4000 Hz. A remarkable response of the flame at twice the forcing frequency is observed at 3000 Hz and 4000 Hz as n_p^{21} are considerably larger than zero at these frequencies. This response at higher frequencies might explain the lower response at the forcing frequency. Furthermore, the constant phase for different excitation frequencies indicates that the time lag is not due to an convective phenomenon. A convective time lag should be independent from the excitation frequency.

5.4.2 Amplitude dependence at 4000 Hz

Test cases 3, 5, 6 and 9 are simulated to study the non-linear behavior of the flame. All test cases have the same forcing frequency of 4000 Hz. As mentioned before, the amplitude of case 9 is linearly increased in time. This has two advantages. First, it does not introduce disturbances at the beginning of the simulation. In simulations with a constant forcing amplitude, either the pressure fluctuations in the domain or the source terms are different to zero at the beginning, as pressure fluctuations and source terms have a phase difference of 90°. This introduces perturbations which excite the eigenfrequencies of the system. Quite long simulations times are necessary to damp out this spurious waves, so that the domain is finally excited only at the desired excitation frequency. By linearly increasing the amplitude, pressure fluctuations and source terms are zero at the beginning and the spurious waves do not appear. This has already been shown by Ducruix ([4]). Furthermore, this linear sweep has the second advantage that the non-linear behavior can be

[ii] P: Pressure excitation; V: Velocity excitation

determined from one single simulation. The main problem is to identify the model parameters very accurately in the case with the time dependent amplitude. A very simple approach is currently used. A transient FFT of the excitation and the response is calculated. For each FFT, a time window of one period of the excitation frequency is analyzed and the amplitude and phase at the excitation frequency are extracted. Figure 7 shows the pressure signal at the outlet and the volume integral of the heat release as a function of time. The linear increase of the pressure amplitude is clearly visible, whereas the flame does not show the same behavior. It is discernible that the mean heat release rate changes with time.

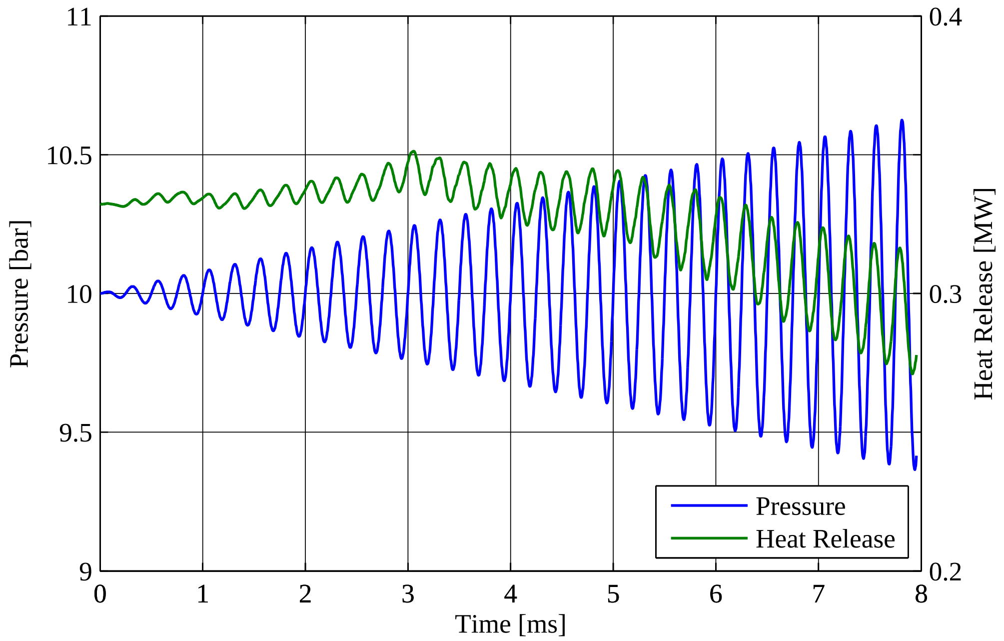

Figure 7: Flame response as function of the pressure amplitude

Figure 8 shows the extracted flame model parameters n and τ as a function of the excitation amplitude. Furthermore, the simulations at a constant amplitude are shown as well. A very good agreement can be observed except for very low amplitudes. The deviation at low amplitudes is due to the fact that the identification is imprecise for the case with the linearly increasing amplitude. The interaction index shows small variations with the amplitude whereas the time lag remains constant in the investigated range. In the future, it will be investigated which slope can be used to get the shortest simulation time and the best possible analysis of the flame. Probably, more elaborated methods have to be used to determine the flame model parameters accurately. The aim is to use mainly the linear increase in the future as it represents the advantages presented above. Furthermore, it is interesting to see the influence of these flame parameter variations with amplitude on the global stability. It is known that a amplitude dependent flame behavior can either lead to non-linear triggering or limit cycles.

5.4.3 Phase shift in axial direction at 4000 Hz

Test cases 3, 5, 7 and 8 are used to study the influence of a phase shift in the axial direction on the flame response. For this purpose, the test case is forced with the previously presented method (cases 3 and 5). Additionally, only the pressure at the outlet fluctuates with the defined frequency and amplitude (cases 7 and 8). This leads to a longitudinal forcing and results in a gradient of the amplitude as well as a phase shift in the axial direction. The mode shape corresponds to a standing longitudinal wave with mean flow. It can be seen from Tab. 2, that the flame response is nearly five times higher with the longitudinal than with the transverse forcing. Axial velocity fluctuations are much higher in the longitudinally forced case, due to the amplitude gradient and the phase shift. This might explain the higher flame

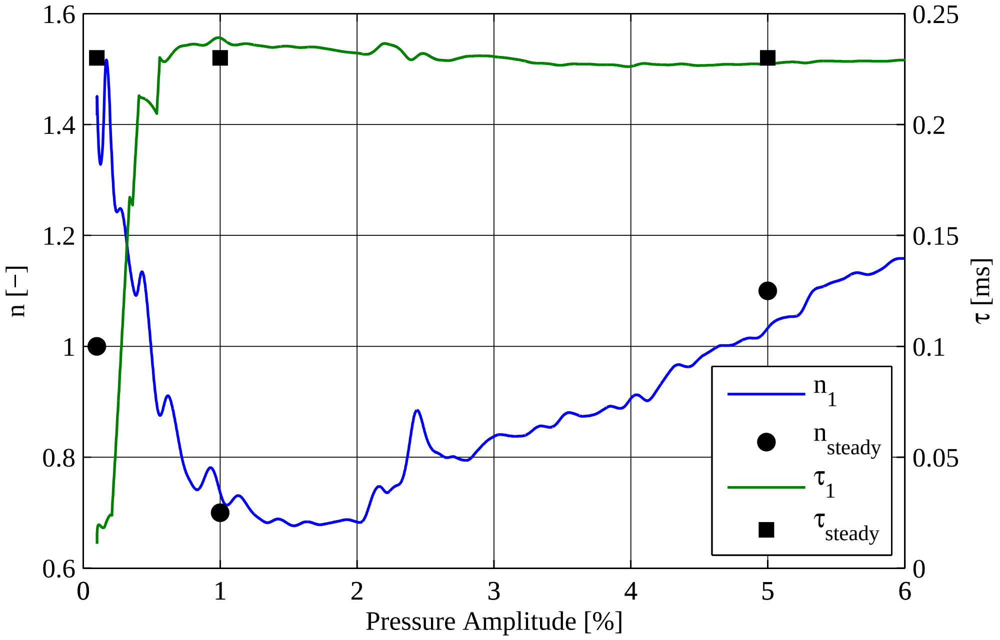

Figure 8: Flame parameters as a function of the excitation amplitude

response, as the flame is much more sensitive to velocity fluctuations than to pressure fluctuations, which are constant in space but fluctuating with time, especially because the combustion model does not account for any influence of pressure on the reaction kinetics. Similar observations can be found in [1] and [6], where the flame response is strongly affected by pressure gradients. There, the influence of gradients on the production of vorticity is studied. Vorticity can be produced due to the misalignment of pressure and density gradients. These effects are very interesting and will be studied in more detail when an excitation method including amplitude gradients and phase shifts is available. The aim is to have a forcing method, which allows full control of the amplitude and phase of the pressure fluctuations in the domain.

5.5 Velocity fluctuations

A second series of test cases studies the influence of velocity fluctuations on the heat release rate. This follows the previously mentioned strategy that the two extreme positions of injectors (pressure and velocity anti-node, see Fig. 6) are of major interest. As already mentioned, a periodically fluctuating force per volume constant in space is applied to excite the velocity fluctuations. The results are also listed in Tab. 2 (simulations 10-15).

5.5.1 Frequency dependence at 0.02% amplitude

Test cases 10-13 have the same excitation amplitude ($\hat{v}\bar{\rho}c/(\bar{p}s_{11}) = 0.02\%$), but different excitation frequencies ranging from 2000 Hz to 5000 Hz. The dimensionless excitation amplitude is quite small compared to the amplitude in the previously presented cases with the pressure excitation method. As already explained, the dimensionless amplitudes can be compared due to the chosen nondimensionalization method. In a dimensional form, the amplitude corresponds to $\hat{v} = 0.5\ m/s$. The flame response intensity and the time lag decrease with increasing excitation frequency. It is observable that the phase remains relatively constant as it is the case with pressure excitation. It can also be seen that the response occurs not at the excitation frequency, but at the double frequency. This behavior is quite intuitive. The flame is rotationally symmetrical around the axis of the injector. Therefore, a forcing to the positive or negative transverse direction should lead to the same response, which finally leads to a global response at twice the excitation frequency. Analogue results have already been observed in [12] and [5]. The authors present a different interpretation of the results, because they consider the local fluctuations, but the global response is also at the double frequency. The global response of an injector is the important one for the feedback mechanism if the injector is much smaller than the acoustic wave length in transverse direction, as it is generally the case in rocket engines.

5.5.2 Amplitude dependence at 3000 Hz and 4000 Hz

Test cases 11 and 14 compare different amplitudes for an excitation frequency of 3000 Hz and test cases 12 and 15 for a frequency of 4000 Hz. The higher amplitude of 0.19% corresponds to a velocity amplitude of $\hat{v} = 5\ m/s$. As before, the flame responds at the double frequency. Some variations of the interaction index with amplitude are visible, but the phase remains approximately the same. This difference in amplitude might be due to non-linear effects or a consequence of the post-processing. For small excitation amplitudes, the response is quite weak and the post-processing is imprecise.
A general remark has to be made on the feedback mechanism in the case of velocity fluctuations. As the flame responds at twice the excitation frequency, the feedback loop cannot be closed. Longitudinal eigenmodes appear at frequencies, which are integer multiples of the fundamental mode. Therefore, a flame response at the double frequency could trigger higher modes. However, transverse eigenfrequencies are not integer multiples. Therefore, velocity fluctuations can even not trigger higher transverse modes.
Schwing [11] recently observed experimentally an unstable transverse mode in the case of a gas turbine burner. This instability could be related to velocity fluctuations. However, there is an important difference to instabilities in rocket engines. The diameter of the investigated burner is in the order of magnitude of the transversal wave length. In contrast, the injector considered in this paper is much smaller than the wave length. This difference explains the different behavior regarding instability and why the feedback loop is closed in the gas turbine burner.

6. Summary and outlook

Numerical excitation methods for acoustic pressure and velocity fluctuations in rocket engine injectors have been presented. They are based on periodically fluctuating source terms on the periodic boundaries (pressure excitation) or in the whole domain (velocity excitation). The influence of these fluctuations on the heat release rate of a gaseous hydrogen/oxygen flame has been computed. Parameters of a n-τ-model for the dynamic flame behavior as a function of the acoustic excitation were identified. One main difference is observed between pressure and velocity fluctuations: The flame responds to pressure excitation at the forcing frequency whereas it responds to velocity fluctuations at twice the excitation frequency. It is also shown that the phase shift in axial direction has an important influence on the response. It is much higher in the case of longitudinal forcing compared to transverse forcing. This indicates an important influence of axial velocity fluctuations on the flame response, even in the case of transverse modes. Furthermore, pressure and velocity fluctuations showed a constant phase for different excitation amplitudes, i.e. no convective phenomenon seems to be responsible for the time lag.
In the future, the presented excitation methods will be used to study gaseous and supercritical flames in more detail, especially the influence of axial velocity fluctuations on the heat release rate. Furthermore, the influence of acoustic fluctuations on the evaporation of liquid droplets of oxygen as well as monomethylhydrazine and dinitrogen tetroxide will be investigated.

7. Acknowledgment

Financial support has been provided by the German Space Agency of *Deutsches Zentrum für Luft- und Raumfahrt e.V.* with funds from the German Federal Ministry of Economics and Technology under grant No. 50RL1040. The authors also acknowledge the support of *EADS Astrium* in Ottobrunn, Germany.

References

[1] K. R. Anderson and S. Mahalingam. Numerical Study of Vortex/Flame Interaction in Actively Forced Confined Non-Premixed Jets. *Journal of Heat Transfer*, 122:376–380, 2000.

[2] L. Crocco and S. Cheng. *Theory of Combustion Instability in Liquid Propellant Rocket Motors*. Butterworths Scientific Publications, 1956.

[3] J. W. Delfs, M. Bauer, R. Ewert, H. A. Grogger, M. Lummer, and T. G. W. Lauke. Numerical Simulation of Aeroacoustic Noise by DLR-s Aeroacoustic Code PIANO. Technical report, DLR Braunschweig, 2002.

[4] S. Ducruix and S. Candel. External Modulation of Confined Flows in Computational Fluid Dynamics. *AIAA Journal*, 42:1550–1558, 2004.

[5] S. Ducruix, C. Rey, and S. Candel. A Method fot the Transverse Modulation of Reactive Flows with Application to Combustion Instability. *Combustion Theory and Modelling*, 9(1):5–22, 2005.

[6] A. Ghosh. *The Role of Density Gradient in Liquid Rocket Engine Combustion Instability*. PhD thesis, University of Maryland, 2008.

[7] J. Görgen, M. Frey, and O. Knab. RCM-2: Rocflam-II Spray Combustion Simulation of the Mascotte 60 bar Combustor. In *3rd International Workshop ROCKET COMBUSTION MODELING*, 2006.

[8] A. Kaufmann, F. Nicoud, and T. Poinsot. Flow Forcing Techniques for Numerical Simulation of Combustion Instabilities. *Combust. and Flame*, 131, 2002.

[9] P.M. Morse and K.U. Ingard. *Theoretical Acoustics*. Princeton University Press, 1968. None.

[10] J. Pieringer. *Simulation selbsterregter Verbrennungsschwingungen in Raketenschubkammern im Zeitbereich*. PhD thesis, Lehrstuhl für Thermodynamik, Technische Universität München, 2008.

[11] J. Schwing, N. Noiray, and T. Sattelmayer. Interaction of Vortex Shedding and Transverse High-frequency Pressure Oscillations in a Tubular Combustion Chamber. In *ASME Turbo Expo: Power for Land, Sea and Air, No. GT2011-45246, Vancouver, Canada*, 2011.

[12] M. Sliphorst, S. Groening, B. Knapp, and M. Oschwald. Combustion Instability Coupling Mechanisms Between Acoustics and LOX/CH4 Spray Flames. In *49th AIAA Aerospace Sciences Meeting including the New Horizons Forum and Aerospace Exposition*, 4-7 January 2011.

[13] Snecma Moteurs, Rocket Engine Division. Test Case RCM-2: Mascotte Single Injector 60 bar. In *3rd International Workshop ROCKET COMBUSTION MODELING*, Vernon, France, 2006.

[14] L. Tay Wo Chong, T. Komarek, R. Kaess, S. Foeller, and W. Polifke. Identification of Flame Transfer Functions from LES of a Premixed Swirl Burner. In *ASME Turbo Expo: Power for Land, Sea and Air, No. GT2010-22769, Glasgow, Scotland*, 2010.

[15] A. Török, J. Steelant, and T. Sattelmayer. CFD Modelling Concept for the Computation of Dynamic Heat Release in Rocket Motors. In *Space Propulsion, San Sebastian, Spain*, 2010.